JCS ePress online publication date 10 February 2012

Identifying a novel functional domain within the p115 tethering factor required for Golgi ribbon assembly and membrane trafficking

Robert Grabski, Zita Balklava[1], Paulina Wyrozumska, Tomasz Szul, Elizabeth Brandon, Cecilia Alvarez[2], Zoe G. Holloway[3] and Elizabeth Sztul

Department of Cell Biology
University of Alabama at Birmingham
Birmingham, AL 35924

[1]School of Life and Health Sciences
Aston University
Birmingham B4 7ET
United Kingdom

[2]Departamento de Bioquimica Clinica, CIBICI-CONICET
Universidad Nacional de Cordoba
Ciudad Universitaria, Cordoba, CP.5000
Argentina

[3]Wellcome Trust Centre for Human Genetics
University of Oxford
Headington, Oxford, OX3 7BN
United Kingdom

corresponding author:
Elizabeth Sztul
Phone: 205- 934-1465
email: esztul@uab.edu

Abstract

The tethering factor p115 has been shown to facilitate Golgi biogenesis and membrane traffic in cells in culture. However, the role of p115 within an intact animal is largely unknown. Here, we document that RNAi-mediated depletion of p115 in *C. elegans* causes accumulation of the yolk protein (YP170) in body cavity and the retention of the yolk receptor RME-2 in the ER and the Golgi within oocytes.

Structure-function analyses of p115 have identified two homology (H1-2) regions within the N-terminal globular head and the coiled-coil 1 (CC1) domain as essential for p115 function. We identify a novel C-terminal domain of p115 as necessary for Golgi ribbon formation and cargo trafficking. We show that p115 mutants lacking the fourth CC domain (CC4) act in a dominant negative manner to disrupt Golgi and prevent cargo trafficking in cells containing endogenous p115. Furthermore, using RNAi-mediated "replacement" strategy we show that CC4 is necessary for Golgi ribbon formation and membrane trafficking in cells depleted of endogenous p115.

p115 has been shown to bind a subset of ER-Golgi SNAREs through CC1 and CC4 domains (Shorter et al., 2002). Our findings show that CC4 is required for p115 function and suggest that both the CC1 and the CC4 SNARE-binding motifs may participate in p115-mediated membrane tethering.

INTRODUCTION

Secretion in eukaryotic cells involves the passage of cargo through a linear assembly of membrane bound compartments and is mediated by vesicular carriers. Transport requires pairing of transport vesicles with the appropriate acceptor membrane. Recognition between a vesicle and a target membrane is mediated by tethering factors and soluble NEM-sensitive factor (NSF) attachment protein (SNAP) receptors (SNAREs). Tethering factors appear to mediate initial, loose association of vesicles and target membranes that is followed by a tighter pairing facilitated by the SNAREs. Despite extensive inquiry, the exact mechanisms of tethering remain poorly characterized.

One of the best-studied tethers is p115 and its yeast homologue Uso1p. Initial studies identified Uso1p as an ER-Golgi transport factor since the temperature sensitive mutant, *uso1-1*, blocks traffic of yeast invertase to the Golgi (Nakajima et al., 1991). Subsequently, Uso1p has been shown to regulate sorting of select proteins into COPII vesicles *in vivo* (Morsomme et al., 2003; Morsomme and Riezman, 2002) and to mediate COPII vesicle tethering to Golgi membranes *in vitro* (Barlowe, 1997).

Mammalian p115 has been implicated in COPII and COPI vesicle tethering. p115 is detected on COPII vesicles and COPII vesicles don't tether to Golgi membranes in the presence of anti-p115 antibodies (Allan et al., 2000; Alvarez et al., 2001). In mammalian cells, COPII vesicles may fuse with each other to form larger structures (perhaps vesicular tubular clusters, VTCs) and p115 appear required for this step since removal of p115 from an *in vitro* assay prevents fusion of COPII vesicles to generate larger intermediates (Bentley et al., 2006).

p115 was initially identified as a cytosolic factor required for COPI vesicle-mediated intra-Golgi transport (Clary and Rothman, 1990; Sapperstein et al., 1995; Waters et al., 1992; Wilson et al., 1992). In agreement, p115 has been detected on isolated COPI vesicles (Malsam et al., 2005) and promotes tethering of COPI vesicles to Golgi membranes *in vitro* (Sonnichsen et al., 1998).

Findings from *in vitro* assays have been supplemented with *in vivo* analyses in insect and mammalian cells. Depletion of p115 in insect cells causes fragmentation of Golgi cisternae (Kondylis and Rabouille, 2003), while inactivation of p115 with antibodies or depletion of p115 from mammalian cells causes fragmentation of Golgi ribbon and the formation of Golgi mini-stacks adjacent to ER exit sites (Alvarez et al., 1999; Guo et al., 2008; Holloway et al., 2007; Nelson et al., 1998; Puthenveedu and Linstedt, 2001; Puthenveedu and Linstedt, 2004; Smith et al., 2009; Sohda et al., 2007; Sohda et al., 2005).

The requirement for p115 in protein trafficking is varied. Mammalian cells depleted of p115 show inhibition of VSV-G traffic during exit from the ER (Puthenveedu and Linstedt, 2004), but trafficking of the transmembrane Delta (ligand of Notch) to the surface of S2 cells (Kondylis and Rabouille, 2003) appears unaffected. Similarly, secretion of soluble proteins is delayed but not inhibited in p115-depleted mammalian cells (Sohda et al., 2007; Sohda et al., 2005). Thus, it appears that p115 exerts a modest effect on trafficking of some proteins and has a more pronounced effect on trafficking of other cargoes, such as VSV-G. Here, we assess p115 function in intact worm, *C. elegans* to show that RNAi-mediated depletion of p115 doesn't inhibit secretion of the soluble YP170 protein from the intestine, but affects the trafficking of the

transmembrane RME-2 yolk receptor in oocytes.

p115 has an N-terminal globular domain that contains 2 homology (H1-2) regions showing high amino acid conservation in all p115 orthologs, followed by a region predicted to form 4 coiled-coil (CC1-CC4) domains and a C-terminal acidic domain (AD) (diagramed in Figure 4). p115 exists *in vivo* as a parallel homo-dimer (Sapperstein et al., 1995). p115 binds a number of cellular proteins including Rab1 GTPase through a region requiring R39 in H1 (An et al., 2009; Beard et al., 2005; Shorter et al., 2002), β-COP through a region requiring E19 in H1 (Guo et al., 2008), COG2 through a region requiring amino acids 200-247 in H2 (Sohda et al., 2007), SNAREs through CC1 and CC4 (Shorter et al., 2002) and GM130 and giantin through AD (Alvarez et al., 2001; Linstedt et al., 2000; Nakamura et al., 1997; Nelson et al., 1998; Sonnichsen et al., 1998). Structure-function studies in which endogenous p115 was replaced with p115 mutant in specific domains show that mutations in H1 or H2 and deletions of H2 and CC1 inhibit p115 function in Golgi biogenesis and/or cargo traffic (Guo et al., 2008; Puthenveedu and Linstedt, 2004; Sohda et al., 2007). Thus, H1, H2 and CC1 represent the known functional domains.

However, the temperature sensitive yeast mutants *uso1-1* and *uso1-11* that contain the entire globular head and CC1 (see Figure 4) are functionally compromised (Seog et al., 1994; Yamakawa et al., 1996). This suggests that the CC2-CC4-AD region missing in *uso1-1* and *uso1-11* might be important for Uso1p and perhaps p115 function. In support, *in vivo* deletion of the C-terminal region from bovine p115 has been reported to inhibit exocytic traffic (Satoh and Warren, 2008).

Here we assessed the ability of p115 lacking various C-terminal domains to sustain Golgi ribbon formation and cargo traffic using overexpression and "replacement" strategy. We show that deletion of the AD doesn't influence p115 function, in support of previous report (Puthenveedu and Linstedt, 2004). We document that p115 constructs missing the C-terminal CC3-CC4-AD or only the CC4-AD are compromised in function. Furthermore, we show that p115 lacking only CC4 is unable to support Golgi ribbon formation and cargo trafficking. Our findings suggest that CC4 represents a novel functional domain in p115. Because CC4 has been shown to bind a subset of SNAREs involved in ER-Golgi traffic, our findings suggest a novel model for p115-mediated membrane tethering.

RESULTS

1. Effects of p115 depletion on Golgi ribbon and cargo traffic

Two siRNA effectively (>75%) depleted p115 from HeLa cells (Figure 1A). siRNA #9 was used in subsequent experiments. The anti-p115 RNAi appears specific because scrambled RNA of the same nucleotide composition does not cause p115 depletion (Figure 1A) and normal levels of non-target GM130, Sly1 and calreticulin are present in p115-depleted cells (Figure 1B).

p115 depletion causes fragmentation of the Golgi ribbon, as evidenced by the relocation of GM130 and giantin from a peri-nuclear structure to punctate elements dispersed throughout the cell (Figure 1C and D; cells marked with asterisks). In most figures we selected fields that contain at least one non-depleted cell among the vast majority of p115-depleted cells. The Golgi fragments appear polarized as shown by the localization of the *cis*-Golgi marker GM130 relative to giantin (Figure 1E) or the TGN marker golgin-245 (Figure 1F). This is in agreement with EM images showing stacks of individual Golgi cisternae in p115-depleted cells (Sohda et al., 2005).

Golgi polarity is believed to arise and be maintained through continuous COPI-mediated recycling of Golgi proteins from distal to proximal cisterna (Losev et al., 2006). In p115-depleted cells, Golgi fragments contain the GBF1 guanine nucleotide exchange factor, an ARF activator shown to regulate COPI function at the ER-Golgi interface (Figure 1H) (Garcia-Mata et al., 2003) and the β-COP component of COPI (Figure 1G). This suggests that COPI-mediated recycling may occur in p115-depleted cells.

p115 has been shown to be required for trafficking of VSV-G (Alvarez et al., 1999; Puthenveedu and Linstedt, 2004). We confirmed this finding by expressing ts045VSV-G in control or p115-depleted cells at the non-permissive temperature and assessing VSV-G traffic after shift to permissive temperature. VSV-G is misfolded and retained within the ER at non-permissive temperature in control and p115-depleted cells (Figure 2A and B). After shifting control cells to the permissive temperature for 2 hours, VSV-G is detected within the Golgi and on the PM (Figure 2C). In contrast, in p115-depleted cells, VSV-G is still predominantly detected within the ER (Figure 2D). Only after 12 hours at the permissive temperature, VSV-G exits the ER and is delivered to Golgi fragments and the PM (Figure 2E).

p115 depletion has minimal effect on trafficking of a soluble form of the transmembrane protein dipeptidyl peptidase IV (DPPIV) (Sohda et al., 2005). However, the "artificial" sDPPIV might not represent an optimal soluble secretory cargo. Thus, we assessed trafficking of a bona-fide secretory protein. We selected cochlin, an extracellular matrix glycoprotein that is efficiently synthesized and secreted from HeLa cells (Grabski et al., 2003). We first show that control and p115-depleted cells secrete analogous subsets of radiolabeled proteins in a pulse-chase experiment (Figure 2F, lanes 1 and 3). A negative control is provided by BFA-treated cells that synthesize but do not secrete proteins (Figure 2F, lane 2). An immunoblot confirms efficient p115 depletion within this experiment (Figure 2G).

Cochlin trafficking was explored in control and p115-depleted cells by pulse-chase experiments. In control cells, cochlin is synthesized as a 60kD peptide (Figure 2H, control panel, band 1) that is rapidly processed to two additional species (bands 2 and 3). Band 3 is resistant to Endo-H digestion ((Grabski et al., 2003) and data not shown), indicating Golgi-mediated

carbohydrate processing. Fully glycosylated cochlin is released from control cells within 30 minutes of pulse and release continues during the chase (Figure 2I). The majority (>75%) of cochlin present at the start of the chase is released from cells within 2 hours of chase.

The same 3 cochlin bands are detected in p115-depleted cells at the beginning of the chase (Figure 2H, RNAi panel). The processing of cochlin in p115-depleted cells may be slower, and the partially glycosylated band 2 is still detectable after 4 hours of chase, at a time when it is not present in control cells. Thus, ER to Golgi trafficking of cochlin may be delayed in p115-depleted cells. Nevertheless, cochlin is detected in medium of p115-depleted cells within 30 minutes of chase (Figure 2I, RNAi panel), and the release continues during the chase. As in control cells, the majority (>78%) of cochlin present at the start of the chase is secreted within 2 hours of chase. Thus, it appears that trafficking of soluble secretory proteins such as cochlin is minimally influenced by p115 depletion.

Together, the Golgi biogenesis and cargo traffic studies define the baseline for examining p115 function in intact animals and in replacement approaches to identify novel functional domains within p115.

2. Effect of p115 depletion in intact animal

Previous studies in *A. thaliana* null for p115 show dwarf but viable plants (Takahashi et al.). In contrast, genetic ablation of p115 in the fly *D. melanogaster* causes embryonic lethality (FlyBase). This suggests that the complex morphogenic events required for animal development require p115 and that p115 function in animals can only be examined by silencing p115 in select tissues or at select times. Thus, we used RNAi-based approach to deplete the worm homologue of p115, referred to as *uso-1* (Kamath and Ahringer, 2003). RNAi in worms most effectively silences gene expression in the intestine and oocytes (Kamath et al., 2003). We first tested whether depletion of *C.elegans* p115 affects secretion of the soluble yolk protein of 170kD (YP170) from the intestine. In wild-type or control RNAi-depleted worms, YP170–GFP can be detected in the intestine where it is synthesized, in the oocytes that endocytose it, and in the developing embryos where it is used as a nutrient (Figure 3A, left image). The majority of YP170-GFP in control worms is detected within oocytes. In *uso-1* depleted worms we observed increased accumulation of YP170-GFP in the intestine (Figure 3A, middle image, arrows). When worms were left to feed on *uso-1* dsRNA for longer time, YP170-GFP progressively accumulated in the body cavity (Figure 3A, right image). Abnormal accumulation of YP170-GFP in the body cavity suggests that YP170-GFP is secreted from intestinal cells, but is not efficiently endocytosed into oocytes.

YP170 is endocytosed into oocytes by the RME-2 yolk receptor. Thus, we tested trafficking of RME-2-GFP in control and *uso-1* depleted worms. In control oocytes, RME-2–GFP is predominantly localized at the plasma membrane and in cortical endosomes (Figure 3B, left image). RNAi-mediated depletion of *uso-1* resulted in 2 types of characteristic trafficking phenotypes (Balklava et al., 2007). In majority of *uso-1* depleted worms, RME-2–GFP increasingly accumulated in the endoplasmic reticulum dispersed throughout the cytoplasm of the oocyte (Figure 3B, middle image). The RME-2-GFP pattern resembled that of the ER marker GFP-SP12 (Figure 3C, left image). Significant number of worms also showed possible Golgi accumulation in punctate structures dispersed in the cytoplasm of oocytes (Figure 3B, right

image). This pattern is analogous to the pattern of the Golgi marker GFP-UGTP-1 (Figure 3C, right image). The intracellular accumulation of RME-2-GFP correlated with reduced RME-2–GFP at the cortex and the cell surface. Thus, it appears that like in mammalian cells, p115 regulates protein transport in worms. Furthermore, in both mammals and worms, p115 depletion appears to inhibit trafficking of transmembrane proteins more than soluble proteins.

3. Effects of p115/1-766 on Golgi ribbon

H1, H2 and CC1 are essential for p115 function (An et al., 2009; Guo et al., 2008; Puthenveedu and Linstedt, 2004; Sohda et al., 2007; Takahashi et al.). A possible role for CC2-CC4-AD was suggested by the *uso1-1* and *uso1-11* yeast mutants that contain intact H1, H2 and CC1 (Figure 4A) but are functionally compromised (Seog et al., 1994) and the finding that deletion of the C-terminal region in bovine p115 inhibits exocytic traffic (Satoh and Warren, 2008). To identify functional domains within the C-terminal region of p115, we generated p115/1-766 that is similar to the yeast *uso1-11* (Figure 4B). Expression of p115/1-766 in cells containing endogenous p115 caused disruption of the Golgi ribbon into punctate fragments (Figure 4F). Only 32% of HeLas expressing p115/1-766 contained morphologically normal Golgi ribbons. This compares to >90% of HeLas expressing full-length p115 containing Golgi ribbons (Figure 4E).

The approximate ratio of p115/1-766 to endogenous p115 in transfected cells was assessed. As shown in Figure 4C, approximately equivalent levels of endogenous p115 and p115/1-766 are detected. Within this experiment, immunofluorescence analysis indicates ~65% transfection rate (not shown). This suggests that within transfected cells, p115/1-766 exceeds the endogenous p115 by ~1.5-fold. This relatively low level of overexpression is sufficient for the dominant negative effect of p115/1-766. Thus, eliminating CC3-CC4-AD appears to inhibit p115 function in Golgi ribbon formation.

The function of p115/1-766 was further explored in replacement assays. The baseline for replacement experiments was established by assessing the phenotype of p115-depleted HeLa cells replaced with full-length rat p115 (our siRNA inhibits synthesis of human but not rat p115). As shown in Figure 4G, Golgi is fragmented in p115-depleted cells (cell marked with asterisk), but can be rescued when such cells are replaced with full-length p115 (cell marked with arrowhead). Replacement of p115-depleted cells with p115/1-959 rescued Golgi ribbon in 83% of cells. In contrast, replacing p115-depleted cells with p115/1-766 does not rescue Golgi architecture (Figure 4H) and only 38% of cells expressing p115/1-766 contain Golgi ribbons.

The ability of the full-length p115 to support Golgi biogenesis and the failure of the p115/1-766 mutant is not due to differences in expression levels. As shown in Figure 4D, full-length p115 and p115/1-766 are expressed in similar amounts. These results suggest that the CC3-CC4-AD region absent in p115/1-766 may be important in p115 function.

4. Effects of p115/1-766 on VSV-G trafficking

The effect of p115/1-766 on VSV-G traffic was first assessed in cells containing endogenous 115. In control cells, VSV-G accumulates within the ER at 42^{o}C (Figure 2A) and after shifting the cells to 32^{o}C for 2 hours is detected at the Golgi and the PM (Figure 2C). In

cells expressing p115/1-766, VSV-G is also detected in the ER after 12 hours at 42°C (Figure 5A). However, shifting such cells to 32°C for 1 hour or 2 hours results in VSV-G trafficking to punctate structures clustered in the peri-nuclear region (Figure 5B-C). VSV-G is not detected on the PM in cells expressing p115/1-766 even after 2 hours, suggesting that p115/1-766 is functionally compromised.

The effect of p115/1-766 on VSV-G traffic without interference from endogenous p115 was assessed in p115-depleted. The baseline for such replacement was provided by trafficking of VSV-G in p115-depleted cells replaced with rat p115. VSV-G is present within the ER of cells incubated at 42°C (Figure 5D). After incubating the cells at 32°C for 2 hours, VSV-G is detected within the Golgi and at the PM (Figure 5F). In p115-depleted cells replaced with p115/1-766 and incubated at 42°C, VSV-G is present within the ER (Figure 5E). After shifting the cells to 32°C for 2 hours, VSV-G is detected within punctate Golgi fragments, but not on the PM (Figure 5G). VSV-G can be detected on the PM after 12 hours at 32°C (Figure 5H). Thus, p115/1-766 is compromised in VSV-G traffic, suggesting that CC3-CC4-AD might be important for p115 function.

5. Effects of p115 constructs with C-terminal deletions on Golgi architecture

p115-1/766 lacks CC3-CC4-AD, and to dissect the importance of these domains we generated p115/1-820 and p115/1-934 (Figure 6A). The functionality of p115/1-820 was tested first. As shown in Figure 6D, this construct acts in a dominant negative manner to disrupt the Golgi when expressed in cells. The disruptive phenotype is not caused by the GFP tag added to the N-terminus of p115/1-820 because expression of full-length p115 tagged with YFP has no effect on Golgi architecture (Figure 4E).

p115/1-820 function was further explored in cells depleted of endogenous p115. When p115-depleted cells are replaced with full-length p115, Golgi ribbon is reformed (see Figure 4G). In contrast, when p115-depleted cells are replaced with p115/1-820, Golgi remain fragmented (Figure 6F). The difference in Golgi reformation is not due to expression levels of the full-length p115 or p115/1-820, because similar amounts of each are detected in cells by immunoblotting (Figure 6B). These results imply that p115/1-820 is compromised in Golgi ribbon formation.

The removal of p115 AD inhibited cargo traffic in one study (Satoh and Warren, 2008), but didn't affect p115 function in another study (Puthenveedu and Linstedt, 2004). To test the role of the AD in our system, we characterized the effect of p115/1-934 (Figure 6A). This construct has been shown not to bind GM130 and giantin (Linstedt et al., 2000). Expression of p115/1-934 in cell containing endogenous p115 doesn't affect Golgi architecture (Figure 6E). Replacing p115-depleted cells with p115/1-934 rescued Golgi ribbon formation (Figure 6G). Expression of p115/1-934 was confirmed by immunoblotting (Figure 6C). Thus, it appears that eliminating the AD is not detrimental to p115 function. The finding that p115/1-934, but not p115/1-820 supports Golgi ribbon formation suggests that the region present in p115//1-934 but absent in p115/1-820, i.e., CC4 might be functionally important.

6. Effects of p115ΔCC4 on Golgi architecture and cargo traffic

To assess the role of CC4 in p115 function, we generated p115ΔCC4 (Figure 6A). Expression of p115ΔCC4 was confirmed by immunoblotting (Figure 6C). This construct acts in a dominant negative manner and disrupts the Golgi when expressed in cells containing endogenous p115 (Figure 7B). Similarly, in p115-depleted cells replaced with p115ΔCC4, the Golgi remains largely fragmented with many elements remaining scattered throughout the cell (Figure 7D). We quantitated Golgi disruption in cells transfected with scrambled RNAi (scr), in p115-depleted cells (RNAi), and in p115-depleted cells replaced with full-length p115 (+1-959), p115ΔCC4 (+ΔCC4), p115/1-820 (+1-820) or p115/1-766 (+1-766). As shown in Figure 7E, only 10% of cells transfected with scrambled RNAi have fragmented Golgi. In contrast, 69% of cells transfected with anti-p115 RNAi have fragmented Golgi. The ~30% of cells containing normal Golgi probably contain residual p115 since our depletions are ~70% effective (see Figure 1A). replacement of p115-depleted cells with full-length p115 almost completely rescues Golgi fragmentation, with only 18% of cells showing Golgi disruption. In contrast, replacement with p115/1-766 doesn't rescue Golgi fragmentation, and the Golgi remains fragmented in 62% of cells. Replacement with p115/1-820 or p115ΔCC4 shows intermediate phenotype, with partial but incomplete rescue. The disruptive phenotype is reduced from 69% to 43% by p115/1-820 and from 69% to 31% by p115ΔCC4, but in both cases doesn't approach the almost complete rescue mediated by full-length p115 (from 69% to 18%). Thus, p115/1-820 and p115ΔCC4 appear compromised in Golgi ribbon formation.

We tested the ability of p115ΔCC4 to support VSV-G traffic in p115-depleted cells. Surface biotinylation was used to quantitate the amount of VSV-G transported to the PM within 2 hours of shift from 42°C to 32°C in cells transfected with scrambled or anti-p115 RNAi, and in p115-depleted cells replaced with p115/1-959 or p115ΔCC4. Cells transfected with scrambled RNAi transported 5.3% of cellular VSV-G to cell surface, while cells transfected with anti-p115 RNAi transported only 1.9% (Figure 7F). Replacement of p115-depleted cells with p115/1-959 rescues VSV-G trafficking and 7.9% of VSV-G reaches the PM. In contrast, replacement with p115ΔCC4 doesn't rescue VSV-G trafficking and only 1.3% of VSV-G is detected on the PM. Together, our findings show that p115ΔCC4 is compromised in Golgi ribbon formation and VSV-G trafficking, and suggest that CC4 is important for p115 function.

7. Interactions of p115 mutants with cellular proteins

The dominant negative effects of p115/1-766, p115/1-820 and p115ΔCC4 could be due to heterodimerization of mutant p115 with endogenous p115 to form inactive complexes. To test heterodimerization, we expressed GFP-p115/1-959 in cells, immunoprecipitated the lysates with anti-GFP antibodies and probed the precipitates for GFP-p115/1-959 and endogenous p115. GFP-p115/1-959 and endogenous p115 are detected in cell lysates (Figure 8A, lane 1) and GFP-p115/1-959 is efficiently immunoprecipitated (lane 2). Significantly, only GFP-p115/1-959 is recovered during immunoprecipitation (lane 3). Immunoprecipitation with non-immune IgG (lanes 4 and 5) confirms specificity of this assay. Thus, it appears that GFP-p115/1-959 and endogenous p115 don't heterodimerize. A possible explanation might be that dimerization occurs

co-translational. An mRNA encoding p115 or GFP-p115/1-959 will be simultaneously translated by numerous ribosomes attached every ~100 base pairs, with proteins on adjacent ribosomes approximately 30 amino acids "apart" in terms of length. Thus, nascent p115 on adjacent ribosomes will have CC1-CC2 regions available for dimerization while the C-terminus is still being translated and are likely to dimerize before being released from the ribosome. The co-translational model of dimerization implies that monomeric p115 is unlikely to be a major cellular component. This indeed appears to be the case since p115 monomers have not been detected in cells (Sapperstein et al., 1995). This also suggests that once formed, homodimers remain stable and don't undergo monomer exchange.

The lack of heterodimerization between GFP-p115/1-959 and endogenous p115 suggested that exogenously expressed mutants also don't dimerize with endogenous p115. We assessed this experimentally by testing heterodimer formation between p115/1-820-myc and endogenous p115. As shown in Figure 8B, lane 3, p115/1-820-myc and endogenous p115 are detected in cell lysates. However, only p115/1-820-myc is recovered after immunoprecipitation with anti-myc antibodies (lane 2). Immunoprecipitation with non-immune IgG doesn't recover p115 or p115/1-820 (lane 1). Thus, exogenously expressed p115 mutants don't form heterodimers with endogenous p115, suggesting that the dominant negative effects of p115 mutants occur without heterodimerization. Instead, it is possible that p115 mutants compete with endogenous p115 for binding to cellular proteins required for trafficking. p115 is a cytoplasmic protein that rapidly cycles on and off membranes in a process regulated by SNAREs binding (Brandon et al., 2006). Thus, it is possible that mutant p115 may compete with endogenous p115 for binding to SNAREs. This model predicts that p115 mutants will associate with membranes and interact with SNAREs.

Membrane association of p115/1-959, p115/1-766 and p115ΔCC4 was tested by cell fractionation. As shown in Figure 8C, p115/1-959, p115/1-766 and p115ΔCC4 are detected in a post-nuclear supernatant (PNS) of transfected cells, and after fractionation are recovered in the cytosolic (Cyt) and total membrane (TM) fractions. Importantly, all p115 constructs appear to associate with membranes to a similar extend, suggesting that like p115/1-959, p115/1-766 and p115ΔCC4 bind efficiently to membrane "receptors", perhaps SNAREs.

p115 interacts with the SNAREs GOS-28, membrin, Ykt6p and syntaxin-5 through CC1 (Shorter et al., 2002). p115/1-766, p115/1-820 and p115ΔCC4 each contain CC1. To assess whether these proteins might exert their dominant negative effects by binding SNAREs, we tested p115/1-820 binding to syntaxin-5. We first show that endogenous p115 within an isolated stacked Golgi (SG) fraction is recovered on GST-syntaxin beads but not on GST beads (Figure 8D, lanes 1-4). Similarly, GFP-p115/1-959 binds to beads containing GST-syntaxin-5 (Figure 8D, lanes 9-12). Importantly, GFP-p115/1-820 also binds GST-syntaxin-5 beads (Figure 8D, lanes 5-8). Thus, p115/1-820 may exert its dominant negative effect by competing with endogenous p115 for binding to p115 partners such as syntaxin-5.

DISCUSSION

We characterized Golgi architecture and cargo traffic in p115-depleted cells to set a baseline for assessing p115 function in intact animals and in replacement assays to identify novel functional domains within p115.

p115 role in Golgi ribbon formation

We and others have shown that Golgi fragments into polarized dispersed structures in p115-depleted cells (Holloway et al., 2007; Puthenveedu and Linstedt, 2001; Puthenveedu and Linstedt, 2004; Smith et al., 2009; Sohda et al., 2007; Sohda et al., 2005). A plausible model for this phenotype is that COPII vesicles continue to bud and fuse to generate larger structures (perhaps VTCs) adjacent to ER exit sites, but that those structures do not mature into transport competent VTCs. Instead, each VTC remains close to ERES and differentiates into a Golgi mini-stack in a manner similar to that observed in nocodazole-treated cells (Miles et al., 2001; Rhee et al., 2005; Storrie, 2005). This model has several implications regarding the tethering function of p115. Transmembrane Golgi proteins continuously cycle between the Golgi and the ER (Miles et al., 2001; Rhee et al., 2005) in a process mediated by COPII vesicles (Peng et al., 1999; Aridor et al., 2001; Powers and Barlowe, 2002; Zeuschner et al., 2006). The formation of Golgi mini-stacks in p115-depleted cells suggests that COPII vesicles can fuse to generate VTCs in the absence of p115. The subcompartment organization of the Golgi depends on the recycling of proteins from distal to proximal cisternae by COPI vesicles (Glick and Nakano, 2009; Storrie, 2005). COPI vesicle traffic between *medial*- and *cis*-Golgi appears to involve p115 interactions with the GM130 and giantin tethers (Sonnichsen et al., 1998). The polarized distribution of proteins within Golgi fragments in p115-depleted cells suggests COPI-mediated recycling. This is supported by the presence of the ARF activator GBF1 and β-COPI coat on Golgi fragments. Thus, p115 might not be absolutely required for COPII and COPI vesicle tethering. We can't exclude that incomplete p115 depletion provides sufficient p115 to facilitate tethering, but studies in plants also suggest that p115 might be dispensable for tethering (which is believed to be an essential process). In plants, genetic ablation of p115 results in dwarf, but viable plants (Takahashi et al.). Thus, p115-mediated tethering might improve the efficiency of trafficking by facilitating more rapid SNARE encounters and more efficient membrane docking and fusion.

Interestingly, findings from *in vivo* studies differ from *in vitro* assays where p115 is absolutely required for fusion of COPII vesicles with Golgi membranes or with each other, and for COPI-mediated intra-Golgi traffic. A possible explanation for this discrepancy may be that *in vivo* phenotypes are based on long-term treatments with siRNA or expression of dominant negative p115 mutants that allow cells to develop compensatory mechanisms. It is also possible that other tethers such as TRAPP and COG substitute for p115 function *in vivo*. Alternatively, *in vivo* studies monitor localization of endogenous Golgi proteins such as giantin and GalNacT, while all *in vitro* studies utilize VSV-G to measure p115 function. p115 depletion strongly inhibits VSV-G trafficking (see below) and this may have influenced interpretation of *in vitro* results.

p115 role in cargo traffic

Trafficking of soluble proteins including sDPPIV (Sohda et al., 2007; Sohda et al., 2005) and cochlin (this study) seems minimally affected by p115 depletion. Both sDPPIV and cochlin show slightly delayed but normal glycosylation, consistent with correct differentiation of Golgi subdomains. Disruption in glycosyltransferase localization (for example by inhibiting COG function) leads to altered glycosylation of cargo proteins (Zolov and Lupashin, 2005). That p115 depletion has limited effect on secretion of soluble cargoes is also supported by findings that the soluble YP170 appears efficiently secreted in p115-depleted *C. elegans*.

A number of transmembrane proteins including giantin, GS27, mannosidase 2, GalNacT, ERGIC53 (Sohda et al., 2007; Sohda et al., 2005), and ATP7A (Holloway et al., 2007) localize to Golgi mini-stacks in p115-depleted cells, suggesting ability to traffic. However, transport kinetics for those proteins haven't been defined, and might be delayed. Here, we show that p115 depletion affects trafficking of the transmembrane RME-2 yolk receptor in intact *C. elegans*.

The limited effect of p115 depletion on secretion of soluble proteins and the moderate effect on some transmembrane proteins contrasts with the strong inhibition in VSV-G traffic. The stage most sensitive to p115 depletion is exit from the ER. This is consistent with the requirement for Uso1p in sorting select cargo proteins for ER exit in yeast (Belden and Barlowe, 1996; Morsomme et al., 2003; Morsomme and Riezman, 2002). The extent to which p115 regulates trafficking of other proteins will require defining the p115-dependent traffic proteome. Overall, it appears that p115 has a differential effect on protein trafficking, and that ER-Golgi transit of select cargoes might be more sensitive to p115 depletion. Thus, p115 may function to sort some cargo proteins in addition to its general role in membrane tethering.

Mapping a novel functional domain within p115

Till now, only the H1, H2 and CC1 have been implicated in p115 function (An et al., 2009; Guo et al., 2008; Puthenveedu and Linstedt, 2004; Sohda et al., 2007). The role of AD is controversial, with one study suggesting that AD is required for cargo trafficking (Satoh and Warren, 2008) while another study documents that AD is dispensable (Puthenveedu and Linstedt, 2004). Our findings that p115/1-934 supports Golgi ribbon formation in p115-depleted cells supports limited role for AD. The discrepancy might be due to the size of the AD truncation. Our p115-1-934 construct removes only AD, while the construct in the Satoh and Warren study generates p115/1-886 and removes not only AD but also 11 amino acids from CC4 (see diagram in Figure 4B). Considering the essential role of CC4 (see below), it is possible that the observed traffic defect is due to disruption of CC4, rather than elimination of AD.

We identified CC4 as a novel functional p115 domain. Our studies were prompted by the functionally compromised *uso1-1* and *uso1-11* mutants (Seog et al., 1994; Yamakawa et al., 1996), and the finding that CC4 interacts with a subset of ER-Golgi SNAREs (Shorter et al., 2002). We generated three C-terminally truncated p115s (p115/1-766, p115/1-820 and p115/1-934) and examined their effect on Golgi ribbon architecture. We show that p115/1-766 and p115/1-820, but not p115/1-934 act as dominant negatives and disrupt Golgi ribbons in cells containing endogenous p115. Furthermore, p115/1-766 and p115/1-820 don't support Golgi ribbon formation when expressed in p115-depleted cells, but p115/1-934 sustains Golgi ribbon formation. These results suggested that CC4 might be important for p115 function. In support,

we showed that p115ΔCC4 acts as a dominant negative to cause Golgi fragmentation in cells containing endogenous p115 and doesn't support Golgi ribbon formation in p115-depleted cells. We also explored the role of p115 C-terminus in cargo traffic. We document that p115/1-766 and p115ΔCC4 are unable to support VSV-G trafficking in cells depleted of endogenous p115. Together, our data suggest that CC4 is essential for p115 function in Golgi ribbon formation and cargo trafficking.

The Golgi disruption and traffic arrest caused by p115ΔCC4 appear similar to those caused by p115ΔCC1 (Puthenveedu and Linstedt, 2004). This similarity suggests that CC1 and CC4 might function at the same stage of trafficking, perhaps to engage partner proteins in a molecular event that results in membrane tethering and fusion. For CC1, these partners might be Rab1 (Beard et al., 2005), Sly1 and the SNAREs syntaxin-5, GOS28, membrin, Ykt6, Sec22, Bet1 and GS15 (Shorter et al., 2002). In contrast, CC4 does not bind Rab1 or Sly1, and interacts with only a subset of SNAREs, namely GOS28, membrin, Ykt6, Bet1 and GS15. A speculative but plausible model for CC1 and CC4 function is to tether membranes by binding SNAREs on opposing membranes. In this model, p115 could bridge membranes by committing one CC to bind the donor membrane while the other CC binds the target membrane. The initial linking function may be followed by p115 promoting SNARE assembly by releasing inhibition or catalyzing SNARE pin formation. p115 appears to preferentially bind to free SNAREs *in vitro* (Bentley et al., 2006) and *in vivo* (Brandon et al., 2006), consistent with a function in facilitating SNARE complex assembly. The four CC regions are separated by proline-rich "hinge" regions that may facilitate rotation relative to the polypeptide backbone. The presence of the hinges has been proposed to facilitate an "accordion-like" collapse of the tether to bring the donor and acceptor membranes into proximity (Yamakawa et al., 1996). Thus, a bridge between two membranes made by CC1 binding to a SNARE on a donor membrane and CC4 binding to a SNARE on a target membrane might undergo collapse to bring the two membranes into close proximity. Our discovery that the SNARE-binding CC4 plays a key role in p115 function will inform future studies aimed at understanding p115-mediated trafficking.

MATERIALS AND METHODS

Worm Strains: *ojIs37 (pie-1p::GFP::ugtp-1)* was obtained from the Caenorhabditis Genetics Centre, *pwIs23(vit-2::GFP*) was a gift from Barth Grant, *pie-1p::GFP::SP12* are described in (Poteryaev *et al*, 2005), *pwIs116(rme-2::GFP)* is described in (Balklava et al., 2007).

RNA interference in worms: *Uso-1* RNAi clone from the Ahringer library (Kamath and Ahringer, 2003) was fed to worms as described (Kamath et al., 2003) with few modifications. Overnight cultures of control (empty L4440 vector) and L4440-*uso-1* containing bacteria were seeded into dishes containing NGM-lite agar medium containing 2mM IPTG and 25 μg ml–1 carbenicillin and induced overnight at room temperature. 30-50 eggs were transferred to the induced plates and following 4 days at 20°C animals were scored as young adults in the P0 generation. Live worms were mounted on 2% agarose pads with 10 mM tetramisole and imaged with a fully motorised Zeiss Axiovert 200M fluorescence microscope (Carl Zeiss Ltd., Welwyn Garden City, UK) and Hamamatsu Orca camera driven by Volocity software (Improvision, Coventry, UK).

Reagents and Antibodies: Restriction enzymes and molecular reagents were from Promega (Madison, WI) or New England BioLabs (Beverly, MA). SuperSignal West Pico Chemiluminescence Substrate, EZ-Link Sulfo-NHS-Biotin reagent, and NeutrAvidin Agarose were from Thermo Fisher Scientific (Rockford, IL).

Rabbit polyclonal antibodies against p115, GM130 and GBF1 have been described (Barroso et al., 1995; Garcia-Mata and Sztul, 2003; Nelson et al., 1998). Monoclonal anti-giantin G1/133 antibody (Linstedt and Hauri, 1993) was from Dr. Hans-Peter Hauri (University of Basel, Basel, Switzerland). The Sly1 polyclonal antibodies were from Dr. Jesse Hay (The University of Montana). The following commercially available antibodies were used: rabbit polyclonal anti-myc (Santa Cruz Biotechnology, Santa Cruz, CA), monoclonal anti-myc and anti-GFP (Invitrogen, Carlsbad, CA), goat anti-rabbit and anti-mouse conjugated with Alexa Fluor 488 and Alexa Fluor 594 (Molecular Probes, Eugene, OR), HRP labeled goat anti-rabbit, goat anti-mouse, and monoclonal anti-Transferrin Receptor (Zymed, San Francisco, CA), rabbit polyclonal anti-β-COP and rabbit polyclonal anti-calreticulin (Affinity BioReagents, Golden, CO), monoclonal anti-GM130 (BD Transduction Laboratories, Lexington, KY), monoclonal anti-Golgin-245 (BD Pharmingen, San Diego, CA), monoclonal anti-β-tubulin (Upstate, Lake Placid, NY) and monoclonal anti-VSV-G (Abcam, Cambridge, MA). 35S-Met/Cys was from MP Biomedicals (Irvine, CA).

Transfection and Immunofluorescence Microscopy: DNA transfections were with TransIT-LT1 Polyamine Transfection Reagents (Mirus Corporation, Madison, WI), according to manufacturer protocols. RNA oligos were transfected with SiLentFect reagent (BioRad, Hercules, CA) according to manufacturer protocol. HeLa cells were cultured and processed for IF as in (Grabski et al., 2003). Fluorescence patterns were visualized with a Leitz Orthoplan epifluorescence microscope (Wetzlar, Germany). Optical sections were captured with a CCD high-resolution camera equipped with a camera/computer interface. Images were analyzed with a power Mac using IPLab Spectrum software (Scanalytics Inc., Fairfax, VA).

DNA and RNA Constructs: The sequences for RNA interference of human p115 were designed by comparing human and rat p115 cDNA. The #9 sequence of 23 nucleotides targeting region 509-531 of human p115 cDNA (**GATTGATGGACTTACTAGCGGAT**; red color indicate

differences in human and rat cDNA) was used to synthesize the sense and anti-sense RNA oligos (IDT, Coralville, IA).

YFP-tagged p115 was generated by PCR and cloning into pEYFP-N1 (Clontech Laboratories, Mountain View, CA), using KpnI/BamHI restriction sites. The GFP-tagged p115/1-820 and p115-959 were cloned into pEGFP-C2 (Clontech) using XhoI/BamHI restriction sites. The GFP-tagged p115/1-766 was cloned into pEGFP-N2 using KpnI/BamHI. The Myc-tagged p115/1-766 was cloned into pcDNA4/TO/Myc-His-A (Invitrogen, Carlsbad, CA) using BamHI/XhoI restriction sites. The Myc-tagged cochlin is described in (Grabski et al., 2003). The p115/ΔCC4 was generated on a backbone of p115/1-820 construct. The 75 nucleotide p115 acidic-tail fragment was added using overlapping PCR, and cloned into the pcDNA4/TO/Myc-His-A vector using BamHI/XhoI restriction sites. The p115/1-934 was generated by PCR and cloned into the pcDNA4/TO/Myc-His-A vector using BamHI/XhoI restriction sites.

Pulse-Chase Metabolic Labeling: Hela cells silenced for 3 days with anti-p115 RNA oligos were co-transfected with myc-tagged cochlin and YFP-p115/1-959 or GFP-p115/1-766. After 24 hrs, cells were subjected to 1 hour starvation with medium lacking Methionine (Met) and Cysteine (Cys) (Mediatech Inc, Birmingham, AL), followed by a 30 min pulse with S^{35}-Met/Cys (MP Biomedicals, Irvine, CA), and chasing for indicated times. Cells were lysed and media were collected at indicated time points. In some experiments, Hela cells silenced for 4 days with anti-p115 RNA oligos cells were treated BFA (5μg/ml, Sigma Chemical Co., St. Louis, MO) for 30 minutes, followed by a pulse-chase as above in the presence of BFA.

Immunoprecipitation, **SDS-PAGE and Immunoblotting:** HeLa cells were solubilized and immmunoprecipitated with anti-myc or anti-GFP antibodies as in (Grabski et al., 2003). Precipitates were analyzed by SDS-PAGE followed by fluorography or transferred to NitroPure nitrocellulose membrane (Micron Separations Inc., Westborough, MA), and subjected to immunoblotting as described (Gao et al., 1998).

GST binding assay: Bacterially expressed GST or a chimera of GST and the cytoplasmic domain of syntaxin-5 were immobilized on SH beads (Amersham Bioscience AB, Uppsala, Sweden). Stacked Golgi fraction prepared as in (Alvarez et al., 1999) or Hela cells transfected with GFP-tagged p115/1-959 or p115/1-820 for 24 hours were lysed in HKM buffer (25mM HEPES pH 7.4, 125mM Potasium Acetate, 5mM Magnesium Acetate, 5% Glycerol, 0.5% Triton X-100, 0.1mM DTT, Protease Inhibitor Cocktail). Beads and lysates were incubated 1 hour at 4°C, centrifuged at 750xg, 4°C for 5 min and beads washed 10 times with HKM buffer. Starting material and bound proteins were separated by SDS-PAGE and immunoblotted with anti-p115 antibodies.

Traffic of VSV-G Protein: HeLa cells were transfected with anti-p115 RNA oligos for 3 days and then transfected with ts045VSV-G-GFP and myc-tagged p115/1-959 or p115/1-766 at non-permissive temperature of 42°C and incubated for ~18 hrs. Cells were shifted to permissive temperature of 32°C and incubated for 2 or 12 hr, fixed and processed for immunofluorescence.

Evaluation of Golgi Morphology: Hela cells transfected with anti-p115 or scrambled RNA oligos for 3 days were transfected with myc-tagged p115/1-959, p115/ΔCC4, p115/1-820 or p115/1-766. After 24 hour, cells were processed for IF with anti-GM130 and anti-myc antibodies. Two microscope coverslips for each condition, repeated three times, were used to count 200 cells

expressing each of the p115 constructs. Golgi morphology was evaluated and analyzed using GraphPad Prism Software (GraphPad Software, Inc., La Jolla, CA). The obtained results were processed using one way ANOVA statistical analysis.

Surface Biotinylation of VSV-G Protein: HeLa cells transfected with anti-p115 or scrambled RNA oligos for 3 days were co-transfected with ts045VSV-G-GFP and Myc-tagged p115/1-959 or p115/ΔCC4, and incubated at non-permissive temperature for ~18 hrs. For each condition cells were processed at t=0h and t=2h after incubation at permissive temperature. Surface biotinylation was according to the manufacturers protocol at 4°C to prevent protein trafficking. After biotinylation, cells were lysed in Buffer A (10 mM HEPES pH 7.4, 150mM NaCl, 1mM $MgCl_2$, 1mM EGTA, +protease inhibitor cocktail), and 50 µg of each lysate was processed for precipitation of biotinylated proteins with 50 µl of NeutrAvidin Agarose (Thermo Fisher Scientific) equilibrated in Buffer A. After washing, NeutrAvidin agarose bound fraction was released in Sample Buffer and processed for SDS-PAGE, and immunoblotting with anti-VSV-G and anti-Transferrin Receptor antibodies. The intensity of VSV-G band was measured using LabWorks software (UVP, Inc., Upland, CA), normalized to the intensity of the signal for Transferrin Receptor, and presented as the % of surface VSV-G relative to total cellular VSV-G.

Cell Fractionation: Hela cells transfected with Myc-tagged p115/1-959, p115/ΔCC4 or p115/1-766 constructs for 2 days, were fractionated as in (Szul et al., 2005). The post-nuclear supernatant (PNS), cytosol (C), and total membrane (TM) fractions were analysed by SDS-PAGE followed by immunoblotting with anti-Myc and anti β-tubulin antibodies.

ACKNOWLEDGEMENTS

We thank Drs. Hans-Peter-Hauri, Jesse Hay, Jennifer Lippincott-Schwartz and Sharon Tooze for gifts of antibodies and plasmids and Dr. Anne Theibert for constructive comments. This work was supported by American Heart Aassociation Grant in Aid (to ES). ZB was supported by the Royal Society Dorothy Hodgkin Fellowship.

FIGURE LEGENDS

Figure 1. Effects of p115 depletion on Golgi ribbon

(A) Cells mock transfected (ctr), transfected with scrambled (scr) RNAi, or with anti-p115 RNAi (#9 and #12) were cultured for 2 or 4 days, lysed, and the lysates immunoblotted with indicated antibodies. Blots were quantitated by densitometry to assess p115 levels (numbers below panel).

(B) Cell lysates from mock transfected cells (ctr) or cells silenced with anti-p115 RNAi for 4 days were immunoblotted with indicated antibodies.

(C-H) Cells silenced with anti-p115 RNAi for 4 days were analysed by IF with indicated antibodies. p115 depletion causes Golgi disruption (C-D). Golgi fragments show polarized localization of GM130, giantin and golgin-245 (E-F). Insets show higher magnification views. GBF1 and COPI are recruited to Golgi fragments (G-H). p115 depleted cells are marked with asterisks. Bars, 10 μm.

Figure 2. Effect of p115 depletion on cargo traffic

(A-E) Mock transfected cells (control) or cells transfected with anti-p115 RNAi for 3 days (RNAi) were transfected with ts045-VSV-G at 42°C and cultured for additional 12 hours (A-B). Cells were shifted to 32°C for indicated times and analysed by IF with indicated antibodies. In control cells, VSV-G traffics to the Golgi and the plasma membrane (C). In p115-depleted cells, VSV-G is largely retained within the ER (D). In p115-depletd cells after 12 hours at 32°C, VSV-G is detected in internal punctate fragments and the PM (E). p115-depleted cells are marked with asterisks. Bars, 10 μm.

(F-G) Untreated cells, cells treated with BFA for 30 minutes and cells silenced with anti-p115 RNAi for 4 days were pulsed with ^{35}S-Met/Cys for 30 minutes and chased with non-radioactive media (with or without BFA) for 1 hour. Equivalent amounts of cell lysates and media were processed by SDS-PAGE and fluorography. Secretion occurs from control and p115-depleted cells, but not from BFA-treated cells (F). p115 depletion was confirmed by immunoblot of cell lysates with indicated antibodies (G).

(H-I) Control cells and cells silenced with anti-p115 RNAi for 3 days were transfected with myc-tagged cochlin for 24 hours, pulsed with ^{35}S-Met/Cys for 30 minutes and chased with non-radioactive media for indicated times. At each time point, media were collected and cells were lysed and subjected to immunoprecipitation with anti-myc. Precipitates were analysed by SDS-PAGE and fluorography. Cochlin is processed and secreted from control and p115-depleted cells.

Figure 3. Effect of p115 depletion in *C. elegans*

(A) Localization of YP170–GFP in control and *uso-1* RNAi-treated animals. YP170–GFP in control RNAi-treated worms is observed in the intestine, the oocytes and embryos. *Uso-1* RNAi-depleted animals show abnormal accumulation of YP170–GFP in the intestine (middle image, arrows) and body cavity (right image, arrowheads). Bar, 50 μm.

(B) Localization of RME-2–GFP in control and *uso-1* RNAi-treated animals. In control worms RME-2–GFP shows predominantly cell surface localization. *Uso-1* RNAi-depleted animals show abnormal accumulation of RME-2–GFP in the ER (middle image, arrows) and the Golgi (right image, arrowheads). Bar, 10 μm.
(C) Localization of the ER marker GFP-SP12 and the Golgi marker GFP-UGTP-1 in oocytes. Bar, 10 μm.

Figure 4. p115/1-766 mutant disrupts Golgi ribbon

(A-B) Diagram of full-length Uso1p and Uso1p encoded by *uso1-1* and *uso1-11*, full-length p115 and p115/1-766. H denotes homology regions between the yeast and mammalian proteins. C denotes coiled-coil regions. AD denotes the acidic domain.

(C) Control cells (lane 2) or cells expressing p115/1-766 (lane 1) were labeled with ^{35}S-met/cys for 18 hours, lysed and lysates immunoprecipitated with anti-p115 antibodies. Precipitates were processed by SDS-PAGE and fluorography. Similar levels of endogenous p115 and of exogenous p115/1-766 are detected.

(D) Control cells (lane 1) or cells silenced with anti-p115 RNAi for 3 days (lanes 2-4) were either mock transfected (lane 2), transfected with YFP-p115/1-959 (lane 3) or myc-p115/1-766 (lane 4) and cultured for additional 18 hours. Cells were lysed and lysates were processed by SDS-PAGE and immunoblotted with indicated antibodies. Cells transfected with anti-p115 RNA oligos show significant depletion of endogenous p115 (lane 2). p115-depleted cells transfected with constructs show robust expression of YFP-p115/1-959 (lane 3) or myc-p115/1-766 (lane 4).

(E-F) Cells transfected with GFP-tagged p115/1-959 or p115/1-766 were analysed by IF with indicated antibodies. Expression of p115/1-959 doesn't alter Golgi morphology (E). Expression of p115/1-766 disrupts Golgi ribbons (F). Bars, 10 μm.

(G-H) Cells silenced with anti-p115 RNAi for 3 days were transfected with YFP-p115/1-959 or myc-p115/1-766, cultured for 18 hours and analysed by IF with anti-GM130 and either YFP fluorescence (G) or anti-myc antibodies (H). Depletion of p115 fragments Golgi ribbon (cells marked with asterisks). Expression of full-length p115 reverses Golgi disruption (G, cell marked with arrowhead). Expression of p115/1-766 does not reverse Golgi disruption (H, cells marked with arrowheads). Bars, 10 μm.

Figure 5. p115/1-766 inhibits VSV-G traffic

(A-C) Cells transfected with GFP-p115/1-766 for 24 hours were transfected with ts045-VSV-G at 42°C, cultured for additional 12 hours and either analysed directly (A) or shifted to 32°C for 1 (B) or 2 hours (C) and processed for IF to detect VSV-G and p115/1-766. VSV-G is largely retained within punctate fragments after 1 (B) and 2 hours at 32°C (C). Bars, 10 μm.

(D-H) Cells silenced with anti-p115 RNAi for 3 days were co-transfected at 42°C with ts045VSV-G and either myc-p115/1-959 (D, F) or myc-p115/1-766 (E, G-H), cultured for additional 12 hours, shifted to 32°C for indicated times and analysed by IF. In p115-depleted cells replaced with full-length p115, VSV-G traffics to the Golgi and the PM (F). In p115-depleted cells replaced with p115/1-766, VSV-G is retained within punctate fragments after 2 hours (G) and after 12 hours (H). Bars, 10 μm.

Figure 6. C-terminal region is required for p115 function

(A) Diagram of full-length and C-terminal p115 mutants.

(B-C) Cells transfected with GFP-tagged p115/1-959 or p115/1-820 (B) or myc-tagged p115/1-934 or p115ΔCC4 (C) for 18 hours were lysed and the lysates were immunoblotted with anti-p115 and anti-β-tubulin antibodies (B) or with anti-myc and anti-β-tubulin antibodies (C). All constructs express the appropriate proteins.

(D-E) Cells transfected with GFP-p115/1-820 or myc-p115/1-934 for 18 hours were analysed by IF with indicated antibodies. Expression of p115/1-820 disrupts Golgi ribbon (D, cell marked with arrowhead). Expression of p115/1-934 has no visible effect on Golgi architecture (E, cell marked with arrowhead). Bars, 10 μm.

(F-G) Cells silenced with anti-p115 RNAi for 3 days were transfected with GFP-p115/1-820 or myc-p115/1-934 for 18 hours, and analysed by IF with indicated antibodies. p115 depletion fragments the Golgi (cell marked with asterisk). Expression of p115/1-820 does not reverse Golgi disruption (F, cell marked with arrowhead). Expression of p115/1-934 reverses Golgi disruption (G, cell marked with arrowhead). Bars, 10 μm.

Figure 7. CC4 is important for p115 function

(A-B) Cells transfected with myc-tagged p115 or p115ΔCC4 for 18 hours were analysed by IF with indicated antibodies. Expression of p115-myc has no visible effect on Golgi architecture (A, cell marked with arrowhead). Expression of p115ΔCC4-myc disrupts Golgi ribbon (B, cell marked with arrowhead). Bars, 10 μm.

(C-D) Cells silenced with anti-p115 RNAi for 3 days were transfected with myc-tagged p115 or p115ΔCC4 for 18 hours, and analysed by IF with indicated antibodies. p115 depletion fragments the Golgi (cell marked with asterisk). Expression of p115-myc reverses Golgi disruption (C, cell marked with arrowhead). Expression of p115ΔCC4-myc doesn't reverse Golgi disruption (D, cell marked with arrowhead). Bars, 10 μm.

(E) Golgi disruption was quantitated in control cells depleted with scrambled RNAi (scr), in cells depleted of endogenous p115 (RNAi) and in cells depleted of endogenous p115 and expressing either myc-tagged full-length p115 (+1-959), p115ΔCC4 (+ΔCC4), p115/1-820 (+1-820) or p115/1-766 (+1-766). The values represent the averages of 3 independent experiments, with more than 50 cells counted each time.

(F) VSV-G traffic was quantitated in cells depleted with scrambled RNAi (scr), depleted of endogenous p115 (RNAi) and depleted of endogenous p115 and replaced with myc-tagged p115/1-959 (+1-959) or p115ΔCC4 (+ΔCC4). The levels of VSV-G present at the PM after a 2 hour shift to permissive temperature is represented as the % of total cellular VSV-G. The values represent the averages of 2 independent experiments.

Figure 8. Interactions of mutant p115 with cellular proteins

(A) Cells transfected with GFP-p115/1-959 for 18 hours were lysed and lysates immunoprecipitated with non-immune or anti-GFP antibodies. The starting material (SM), non-bound fractions (NB) and bound precipitates (B) were analyzed by SDS-PAGE and immunoblotted with anti-p115 antibodies. Similar levels of endogenous p115 and GFP-p115/1-959 are present in the SM (lane 1). GFP-p115/1-959 is depleted from the NB fraction (lane 2). Only GFP-p115/1-959 is recovered in the precipitate (lane 3).

(B) Cells transfected with myc-p115/1-820 for 18 hours were lysed and the lysates immunoprecipitated with non-immune (lane 1) or anti-myc (lane 2) antibodies. The starting material (lane 3) and precipitates were analyzed by SDS-PAGE and immunoblotted with anti-p115 antibodies. Similar levels of endogenous p115 and myc-p115/1-820 are present in SM (lane 3). Only myc-p115/1-820 is recovered in the precipitate (lane 2).

(C) Cells transfected with myc-tagged p115/1-959, p115ΔCC4 or p115/1-766 for 18 hours were fractionated to generate a post-nuclear supernatant (PNS) which was subsequently fractionated into cytosol (Cyt) and total membranes (TM). Similar levels of p115/1-959, p115ΔCC4 and p115/1-766 associate with membranes.

(D) GST or GST with the cytoplasmic domain of syntaxin-5 were incubated with solubilized stacked Golgi (SG) fraction (lanes 1-4), lysate from cells transfected with GFP-p115/1-820 (lanes 5-8), or with GFP-p115/1-959 (lanes 9-12). Bound proteins were eluted and analysed by SDS-PAGE and immunoblotting with anti-p115 antibodies. The starting material for each binding is shown (lanes 1-2, 5-6, and 9-10). Full-length p115/1-959 and p115/1-820 bind to beads containing syntaxin-5 (lanes 4, 8 and 12).

REFERENCES

Allan, B. B., Moyer, B. D. and Balch, W. E. (2000). Rab1 recruitment of p115 into a cis-SNARE complex: programming budding COPII vesicles for fusion. *Science* **289**, 444-8.

Alvarez, C., Fujita, H., Hubbard, A. and Sztul, E. (1999). ER to Golgi transport: Requirement for p115 at a pre-Golgi VTC stage. *J Cell Biol* **147**, 1205-22.

Alvarez, C., Garcia-Mata, R., Hauri, H. P. and Sztul, E. (2001). The p115-interactive proteins GM130 and giantin participate in endoplasmic reticulum-Golgi traffic. *J Biol Chem* **276**, 2693-700.

An, Y., Chen, C. Y., Moyer, B., Rotkiewicz, P., Elsliger, M. A., Godzik, A., Wilson, I. A. and Balch, W. E. (2009). Structural and functional analysis of the globular head domain of p115 provides insight into membrane tethering. *J Mol Biol* **391**, 26-41.

Balklava, Z., Pant, S., Fares, H. and Grant, B. D. (2007). Genome-wide analysis identifies a general requirement for polarity proteins in endocytic traffic. *Nat Cell Biol* **9**, 1066-73.

Barlowe, C. (1997). Coupled ER to Golgi transport reconstituted with purified cytosolic proteins. *J Cell Biol* **139**, 1097-108.

Beard, M., Satoh, A., Shorter, J. and Warren, G. (2005). A cryptic rab1-binding site in the p115 tethering protein. *J Biol Chem*.

Belden, W. J. and Barlowe, C. (1996). Erv25p, a component of COPII-coated vesicles, forms a complex with Emp24p that is required for efficient endoplasmic reticulum to Golgi transport. *J Biol Chem* **271**, 26939-46.

Bentley, M., Liang, Y., Mullen, K., Xu, D., Sztul, E. and Hay, J. C. (2006). SNARE status regulates tether recruitment and function in homotypic COPII vesicle fusion. *J Biol Chem* **281**, 38825-33.

Brandon, E., Szul, T., Alvarez, C., Grabski, R., Benjamin, R., Kawai, R. and Sztul, E. (2006). On and Off Membrane Dynamics of the Endoplasmic Reticulum-Golgi Tethering Factor p115 In Vivo. *Mol Biol Cell* **17**, 2996-3008.

Clary, D. O. and Rothman, J. E. (1990). Purification of three related peripheral membrane proteins needed for vesicular transport. *J Biol Chem* **265**, 10109-17.

Garcia-Mata, R., Szul, T., Alvarez, C. and Sztul, E. (2003). ADP-ribosylation factor/COPI-dependent events at the endoplasmic reticulum-Golgi interface are regulated by the guanine nucleotide exchange factor GBF1. *Mol Biol Cell* **14**, 2250-61.

Glick, B. S. and Nakano, A. (2009). Membrane traffic within the Golgi apparatus. *Annu Rev Cell Dev Biol* **25**, 113-32.

Grabski, R., Szul, T., Sasaki, T., Timpl, R., Mayne, R., Hicks, B. and Sztul, E. (2003). Mutations in COCH that result in non-syndromic autosomal dominant deafness (DFNA9) affect matrix deposition of cochlin. *Hum Genet* **113**, 406-16.

Guo, Y., Punj, V., Sengupta, D. and Linstedt, A. D. (2008). Coat-tether interaction in Golgi organization. *Mol Biol Cell* **19**, 2830-43.

Holloway, Z. G., Grabski, R., Szul, T., Styers, M. L., Coventry, J. A., Monaco, A. P. and Sztul, E. (2007). Activation of ADP-ribosylation factor regulates biogenesis of the ATP7A-containing trans-Golgi network compartment and its Cu-induced trafficking. *Am J Physiol Cell Physiol* **293**, C1753-67.

Kamath, R. S. and Ahringer, J. (2003). Genome-wide RNAi screening in Caenorhabditis elegans. *Methods* **30**, 313-21.

Kamath, R. S., Fraser, A. G., Dong, Y., Poulin, G., Durbin, R., Gotta, M., Kanapin, A., Le Bot, N., Moreno, S., Sohrmann, M. et al. (2003). Systematic functional analysis of the Caenorhabditis elegans genome using RNAi. *Nature* **421**, 231-7.

Kondylis, V. and Rabouille, C. (2003). A novel role for dp115 in the organization of tER sites in Drosophila. *J Cell Biol* **162**, 185-98.

Linstedt, A. D., Jesch, S. A., Mehta, A., Lee, T. H., Garcia-Mata, R., Nelson, D. S. and Sztul, E. (2000). Binding relationships of membrane tethering components. The giantin N terminus and the GM130 N terminus compete for binding to the p115 C terminus. *J Biol Chem* **275**, 10196-201.

Losev, E., Reinke, C. A., Jellen, J., Strongin, D. E., Bevis, B. J. and Glick, B. S. (2006). Golgi maturation visualized in living yeast. *Nature* **441**, 1002-6.

Malsam, J., Satoh, A., Pelletier, L. and Warren, G. (2005). Golgin tethers define subpopulations of COPI vesicles. *Science* **307**, 1095-8.

Miles, S., McManus, H., Forsten, K. E. and Storrie, B. (2001). Evidence that the entire Golgi apparatus cycles in interphase HeLa cells: sensitivity of Golgi matrix proteins to an ER exit block. *J Cell Biol* **155**, 543-55.

Morsomme, P., Prescianotto-Baschong, C. and Riezman, H. (2003). The ER v-SNAREs are required for GPI-anchored protein sorting from other secretory proteins upon exit from the ER. *J Cell Biol* **162**, 403-12.

Morsomme, P. and Riezman, H. (2002). The Rab GTPase Ypt1p and tethering factors couple protein sorting at the ER to vesicle targeting to the Golgi apparatus. *Dev Cell* **2**, 307-17.

Nakajima, H., Hirata, A., Ogawa, Y., Yonehara, T., Yoda, K. and Yamasaki, M. (1991). A cytoskeleton-related gene, uso1, is required for intracellular protein transport in Saccharomyces cerevisiae. *J Cell Biol* **113**, 245-60.

Nakamura, N., Lowe, M., Levine, T. P., Rabouille, C. and Warren, G. (1997). The vesicle docking protein p115 binds GM130, a cis-Golgi matrix protein, in a mitotically regulated manner. *Cell* **89**, 445-55.

Nelson, D. S., Alvarez, C., Gao, Y. S., Garcia-Mata, R., Fialkowski, E. and Sztul, E. (1998). The membrane transport factor TAP/p115 cycles between the Golgi and earlier secretory compartments and contains distinct domains required for its localization and function. *J Cell Biol* **143**, 319-31.

Puthenveedu, M. A. and Linstedt, A. D. (2001). Evidence that Golgi structure depends on a p115 activity that is independent of the vesicle tether components giantin and GM130. *J Cell Biol* **155**, 227-38.

Puthenveedu, M. A. and Linstedt, A. D. (2004). Gene replacement reveals that p115/SNARE interactions are essential for Golgi biogenesis. *Proc Natl Acad Sci U S A* **101**, 1253-6.

Rhee, S. W., Starr, T., Forsten-Williams, K. and Storrie, B. (2005). The Steady-State Distribution of Glycosyltransferases Between the Golgi Apparatus and the Endoplasmic Reticulum is Approximately 90:10. *Traffic* **6**, 978-90.

Sapperstein, S. K., Walter, D. M., Grosvenor, A. R., Heuser, J. E. and Waters, M. G. (1995). p115 is a general vesicular transport factor related to the yeast endoplasmic reticulum to Golgi transport factor Uso1p. *Proc Natl Acad Sci U S A* **92**, 522-6.

Satoh, A. and Warren, G. (2008). In situ cleavage of the acidic domain from the p115 tether inhibits exocytic transport. *Traffic* **9**, 1522-9.

Seog, D. H., Kito, M., Yoda, K. and Yamasaki, M. (1994). Uso1 protein contains a coiled-coil rod region essential for protein transport from the ER to the Golgi apparatus in Saccharomyces cerevisiae. *J Biochem (Tokyo)* **116**, 1341-5.

Shorter, J., Beard, M. B., Seemann, J., Dirac-Svejstrup, A. B. and Warren, G. (2002). Sequential tethering of Golgins and catalysis of SNAREpin assembly by the vesicle-tethering protein p115. *J Cell Biol* **157**, 45-62.

Smith, R. D., Willett, R., Kudlyk, T., Pokrovskaya, I., Paton, A. W., Paton, J. C. and Lupashin, V. V. (2009). The COG complex, Rab6 and COPI define a novel Golgi retrograde trafficking pathway that is exploited by SubAB toxin. *Traffic* **10**, 1502-17.

Sohda, M., Misumi, Y., Yoshimura, S., Nakamura, N., Fusano, T., Ogata, S., Sakisaka, S. and Ikehara, Y. (2007). The interaction of two tethering factors, p115 and COG complex, is required for Golgi integrity. *Traffic* **8**, 270-84.

Sohda, M., Misumi, Y., Yoshimura, S., Nakamura, N., Fusano, T., Sakisaka, S., Ogata, S., Fujimoto, J., Kiyokawa, N. and Ikehara, Y. (2005). Depletion of vesicle-tethering factor p115 causes mini-stacked Golgi fragments with delayed protein transport. *Biochem Biophys Res Commun* **338**, 1268-74.

Sonnichsen, B., Lowe, M., Levine, T., Jamsa, E., Dirac-Svejstrup, B. and Warren, G. (1998). A role for giantin in docking COPI vesicles to Golgi membranes. *J Cell Biol* **140**, 1013-21.

Storrie, B. (2005). Maintenance of Golgi apparatus structure in the face of continuous protein recycling to the endoplasmic reticulum: making ends meet. *Int Rev Cytol* **244**, 69-94.

Takahashi, H., Tamura, K., Takagi, J., Koumoto, Y., Hara-Nishimura, I. and Shimada, T. MAG4/Atp115 is a golgi-localized tethering factor that mediates efficient anterograde transport in Arabidopsis. *Plant Cell Physiol* **51**, 1777-87.

Waters, M. G., Clary, D. O. and Rothman, J. E. (1992). A novel 115-kD peripheral membrane protein is required for intercisternal transport in the Golgi stack. *J Cell Biol* **118**, 1015-26.

Wilson, D. W., Whiteheart, S. W., Wiedmann, M., Brunner, M. and Rothman, J. E. (1992). A multisubunit particle implicated in membrane fusion. *J Cell Biol* **117**, 531-8.

Yamakawa, H., Seog, D. H., Yoda, K., Yamasaki, M. and Wakabayashi, T. (1996). Uso1 protein is a dimer with two globular heads and a long coiled-coil tail. *J Struct Biol* **116**, 356-65.

Zolov, S. N. and Lupashin, V. V. (2005). Cog3p depletion blocks vesicle-mediated Golgi retrograde trafficking in HeLa cells. *J Cell Biol* **168**, 747-59.

Figure 1

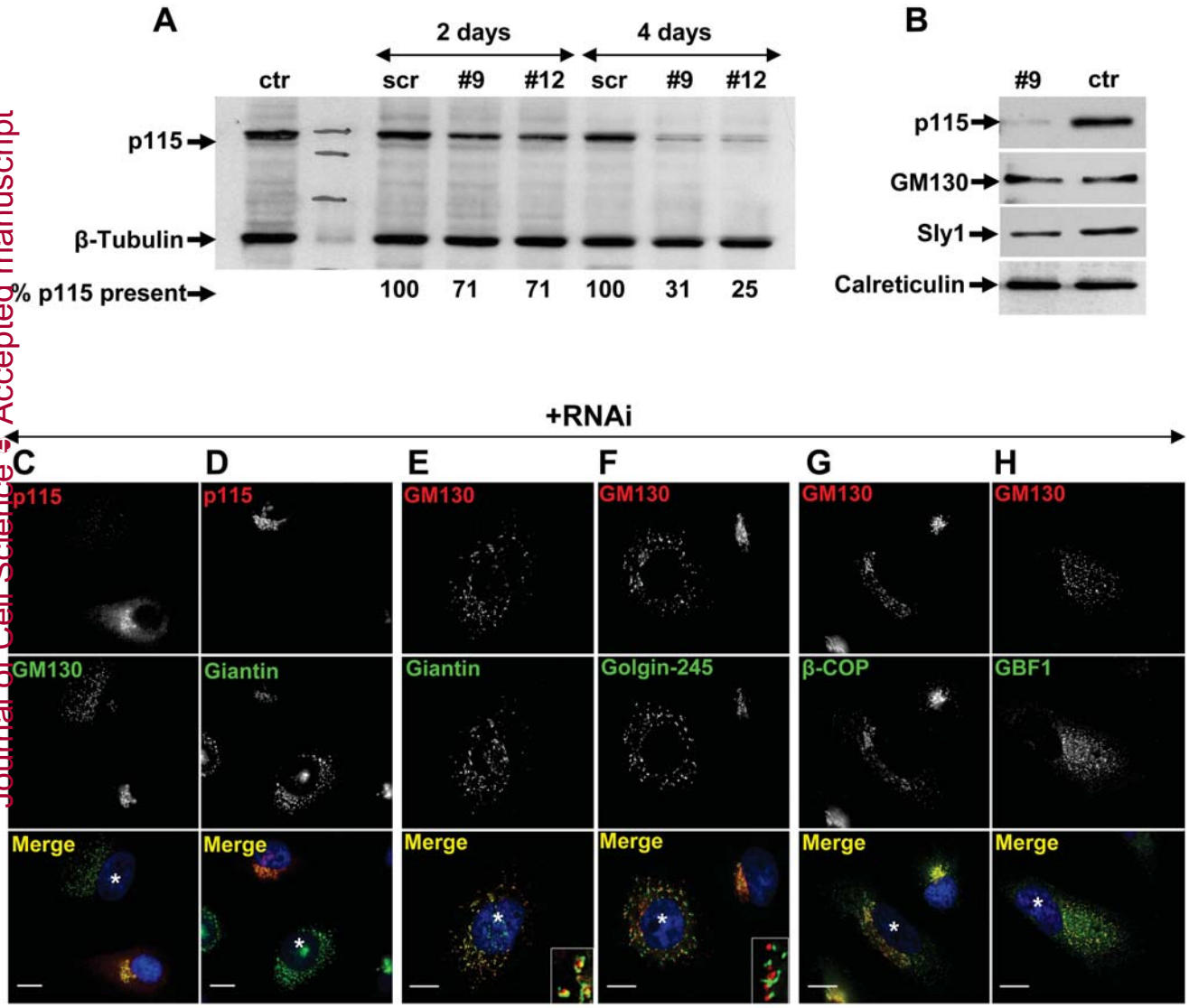

Figure 2

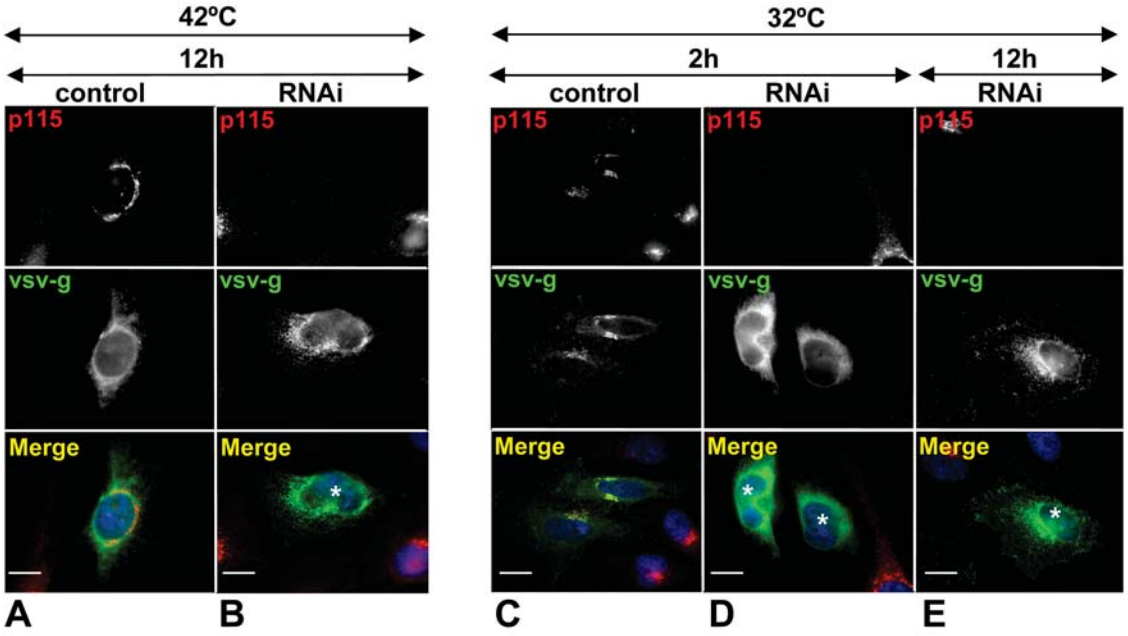

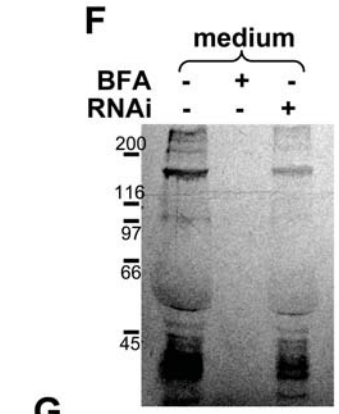

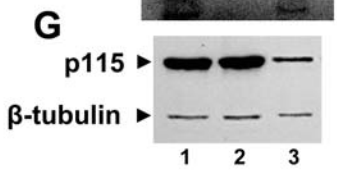

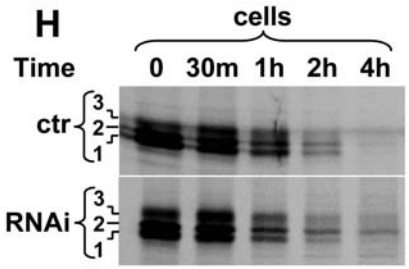

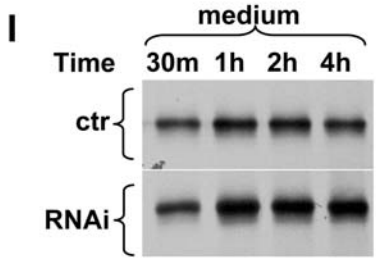

Figure 3

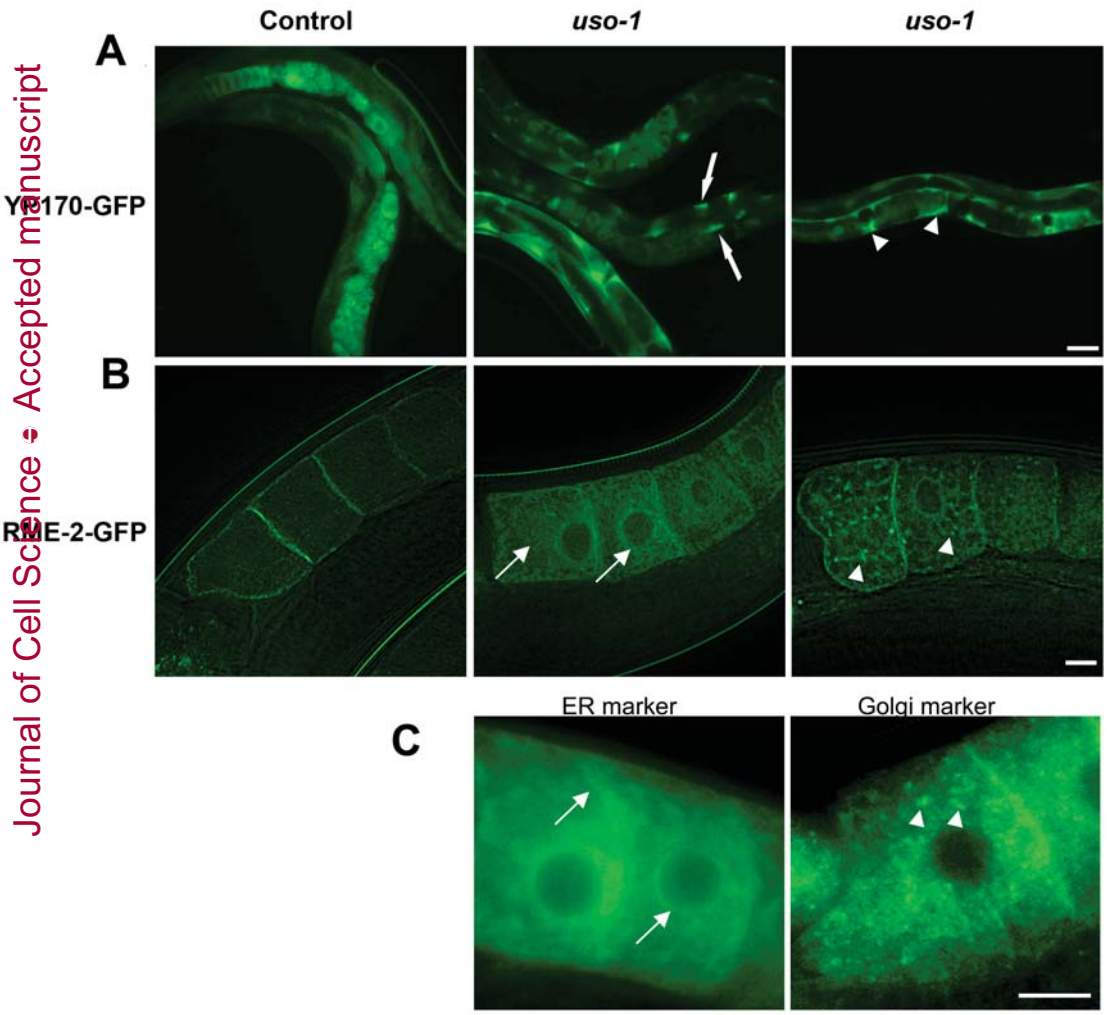

Figure 4

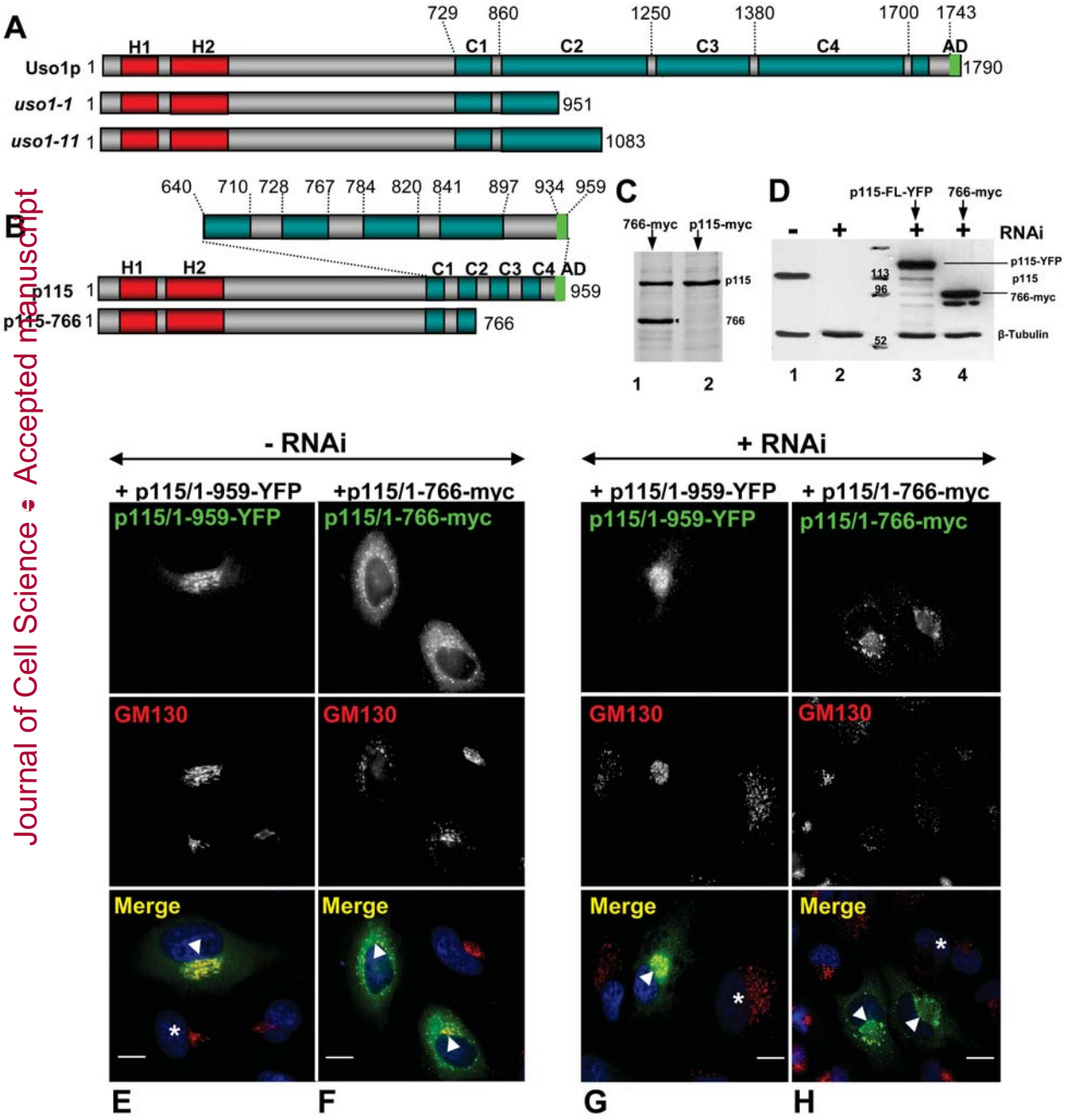

Figure 5

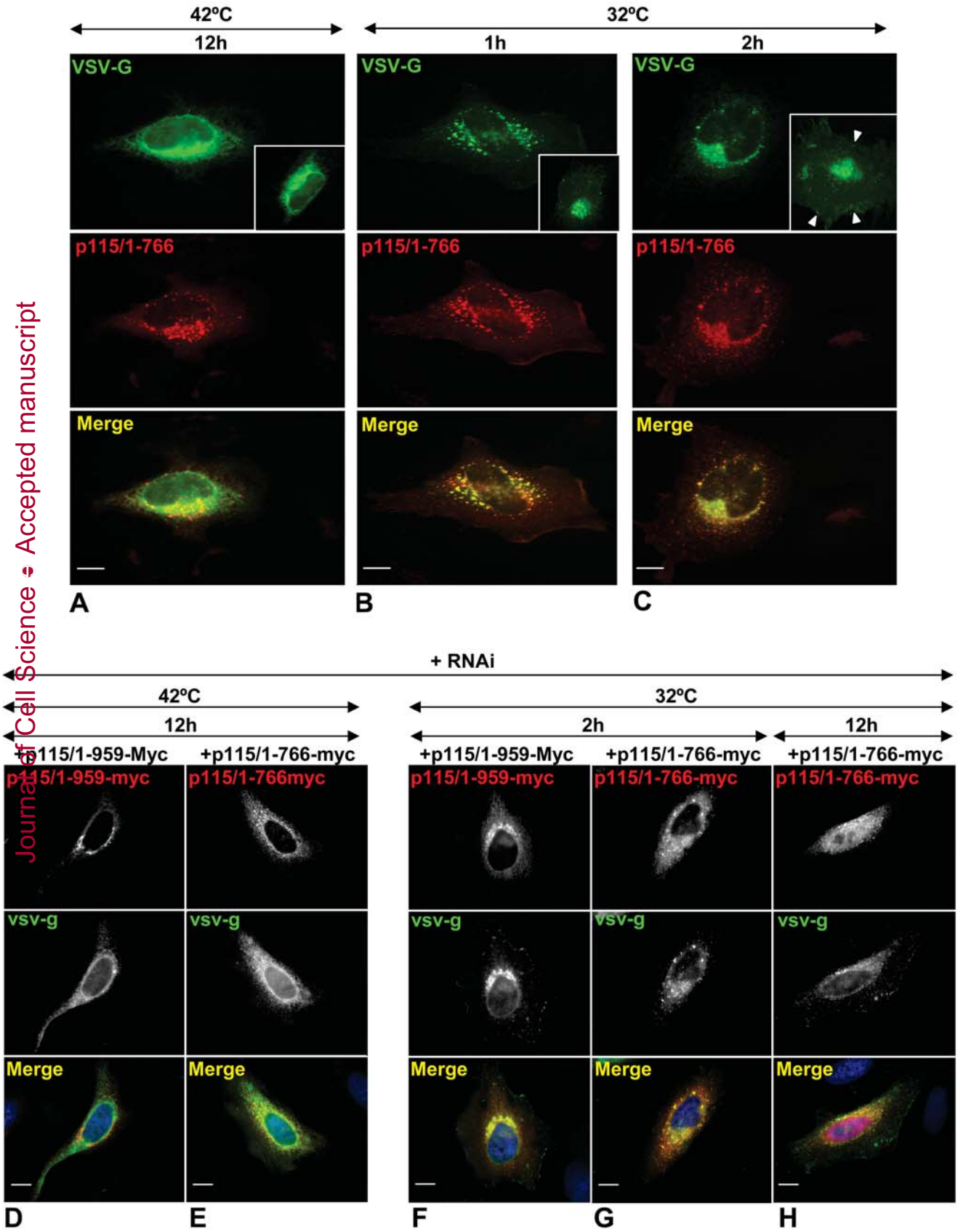

Figure 6

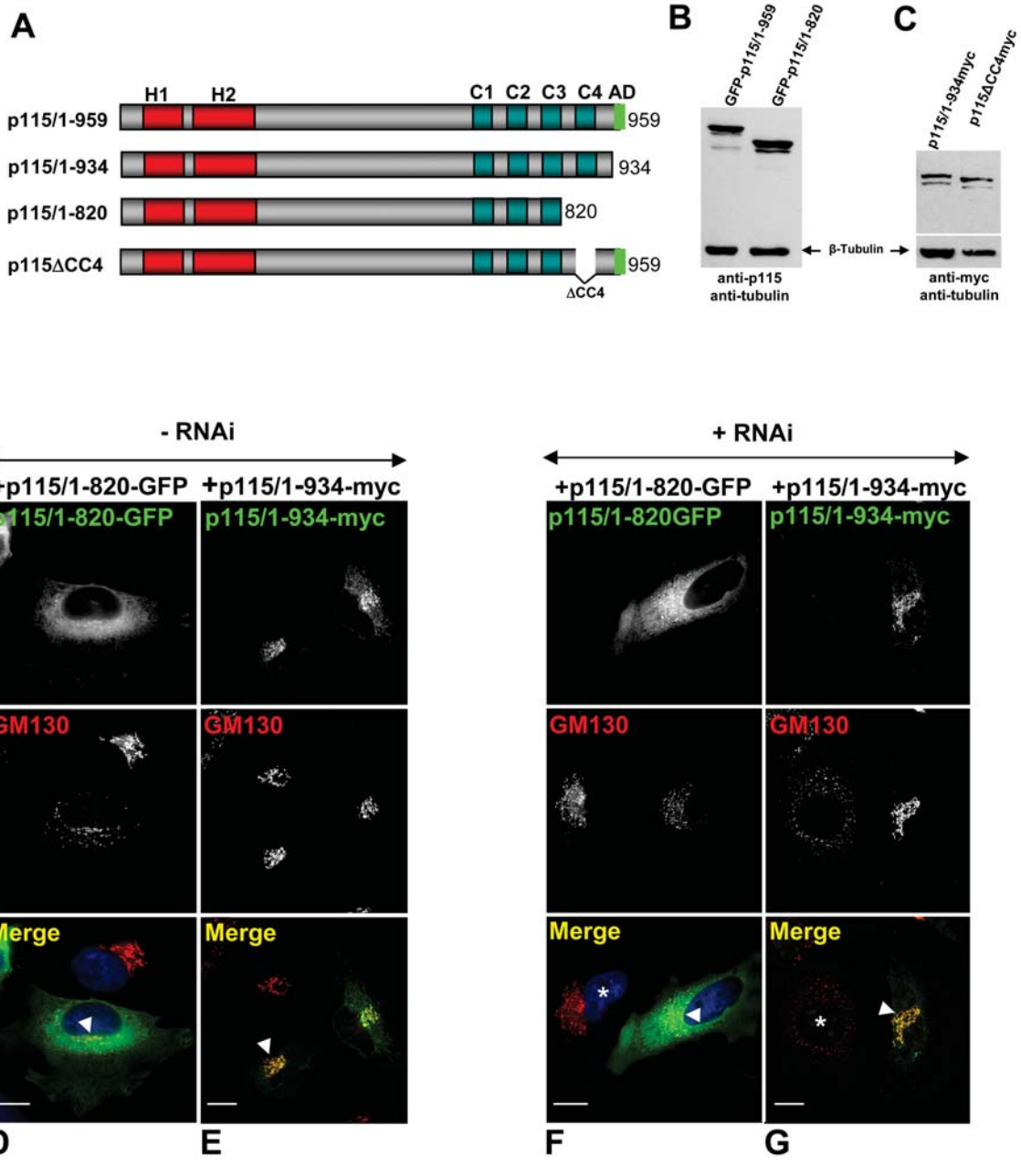

Figure 7

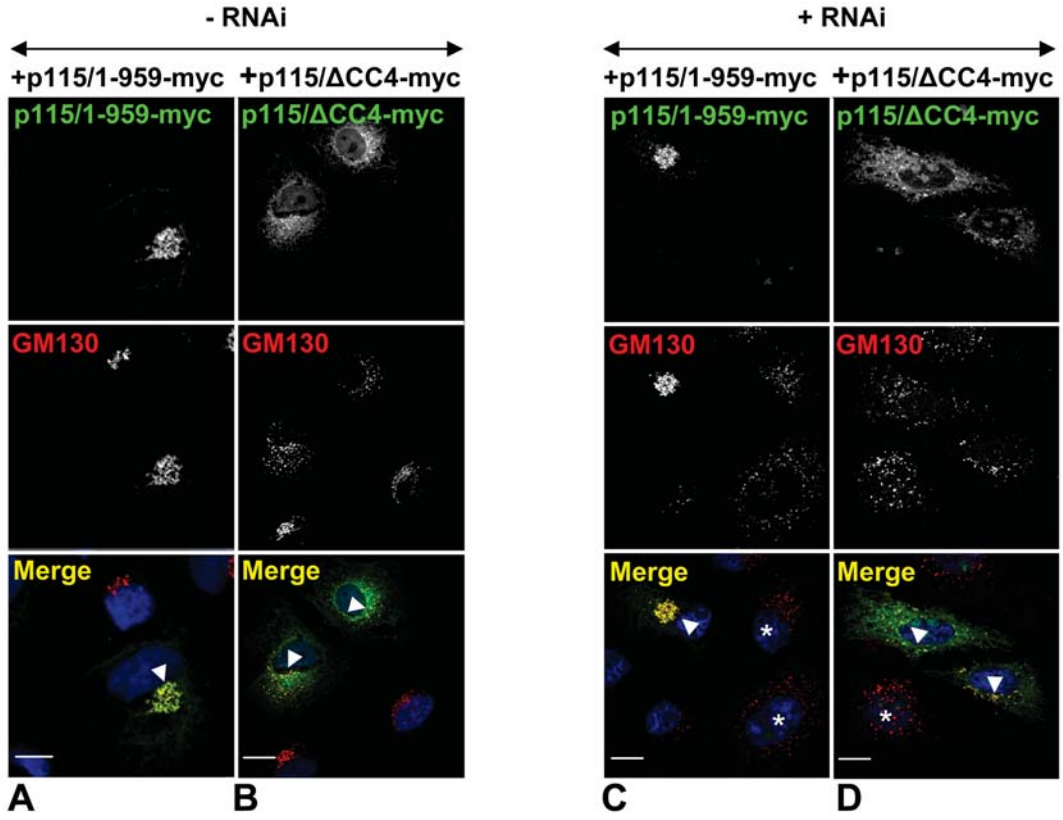

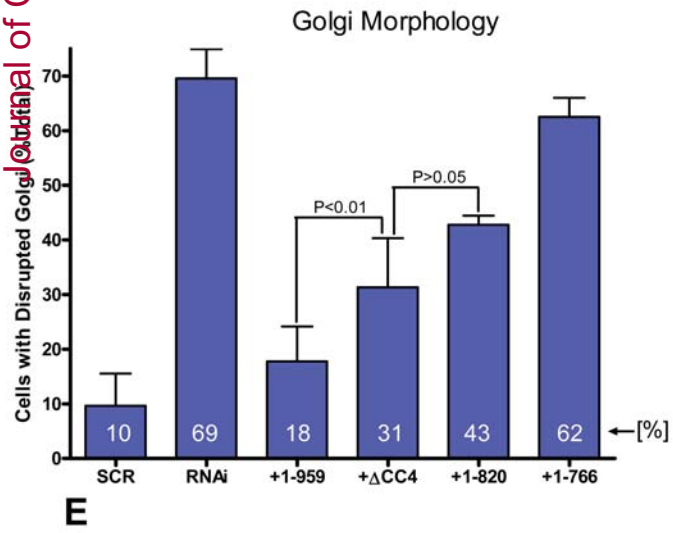

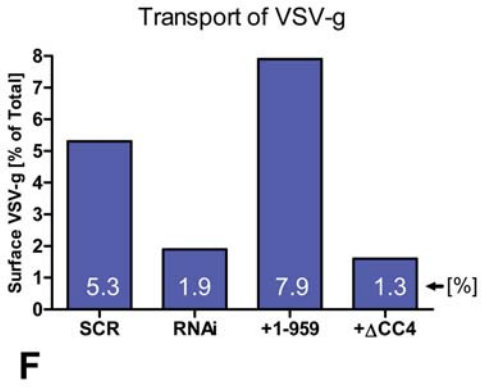

Figure 8